

# PV Ceph: Young Star Caught Speeding?

Alyssa A. Goodman

Harvard-Smithsonian Center for Astrophysics, Cambridge, MA 02138

`agoodman@cfa.harvard.edu`

Héctor G. Arce

California Institute of Technology, Pasadena, CA

`harce@astro.caltech.edu`

Received \_\_\_\_\_; accepted \_\_\_\_\_

## ABSTRACT

Three independent lines of evidence imply that the young star PV Ceph is moving at roughly  $20 \text{ km s}^{-1}$  through the interstellar medium. The first, and strongest, suggestion of motion comes from the geometry of the HH knots in the “giant” Herbig-Haro (HH) flow associated with PV Ceph. Bisectors of lines drawn between pairs of knots at nearly equal distances from PV Ceph imply an E-W motion of the source, and a plasmon model fit to the knot positions gives a good fit of  $22 \text{ km s}^{-1}$  motion for the star. The second bit of damning evidence comes from a redshifted “trail” of molecular gas, pointing in the *same E-W direction* implied by the HH knot geometry. The third exhibit we offer in accusing PV Ceph of speeding involves the tilt apparent in the high-velocity molecular jet now emanating from the star. This tilt is best explained if the true, current, jet direction is N-S, as it is in HST WFPC2 images, and the star is moving—again at roughly  $20 \text{ km s}^{-1}$ .

Tracing the motion of PV Ceph backward in time, to the nearest cluster from which it might have been ejected, we find that it is very likely to have been thrown out of the massive star-forming cluster NGC 7023—more than 10 pc away. PV Ceph and NGC 7023 are at similar distances, and the backward-trace of PV Ceph’s motion is astonishingly well-aligned with a dark, previously unexplained, rift in NGC 7023. We propose that PV Ceph was ejected, at a speed large enough to escape NGC 7023, at least 100,000 years ago, but that it did not enter the molecular cloud in which it now finds itself until more like 35,000 years ago. Our calculations show that currently-observable molecular outflow associated with PV Ceph is about 10,000 years old, so that the flow has had plenty of time to form while in its current molecular cloud. But, the question of what PV Ceph was doing, and what gas/disk it took along with it in the time it was traveling

through the low-density region between NGC 7023 and its current home is open to question.

Recent numerical simulations have suggested that condensed objects should be ejected at high velocity before they have “finished” forming in a cluster. Prior to this work, a handful of pre-main-sequence stars have been shown to be moving at speeds  $> 10 \text{ km s}^{-1}$ . To the best of our knowledge, though, the analysis of PV Cep and NGC 7023 described here is the first observational work associating a speeding young star with a distant ancestral cluster. These high-speed ejections from clusters will create a class of rapidly-moving young stars in molecular clouds. If these ejections are at all common, their existence confounds both calculations of clouds’ star-forming efficiency and theories of star formation that do not allow for stars to move rapidly through a reservoir of star-forming material while they form.

*Subject headings:* stars: kinematics — stars: formation — ISM: jets and outflows — ISM: Herbig-Haro objects — stars: individual (PV Cephei) — ISM: individual (HH 315)

## 1. Introduction

The “knots” evident in HH flows from young stars come in pairs located at similar (but not necessarily exactly equal) distances from the powering star. It is ordinarily presumed, and we agree, that diametrically opposed knots at roughly equal distance from the star are created together. Each knot shows the position of a shock caused by the interaction of ejecta from the young star with its environment. Much evidence—including the prevalence of multiple knot pairs in HH flows—points to the flows being highly episodic (e.g., Arce & Goodman 2001; Reipurth & Bally 2001). The episodicity is probably the result of sporadic accretion onto the young star. Thus, as Bo Reipurth has emphasized, the knots represent a “fossil record” of a young star’s accretion history. In this paper, we use this fossil record in a new way—to track the motion of the young star. Our principal result is the mildly dramatic suggestion that the Young Star PV Cephei is moving at roughly  $20 \text{ km s}^{-1}$  through the interstellar medium.

PV Ceph is a Herbig Ae/Be star (Li, Evans, Harvey, & Colome 1994) located about 500 pc from the Sun (Cohen, Kuhl, Spinrad, & Harlan 1981). The “giant” Herbig-Haro flow from PV Ceph, which extends for more than a pc on the sky, was first mapped optically by Reipurth, Bally, & Devine (1997) and Gómez, Kenyon, & Whitney (1997), and the molecular outflow associated with that flow has been extensively studied by Arce & Goodman (2002a,b). The source is a favorite of amateur optical astronomers, because the nebulosity (known as GM29 or “Gyulbudagyan’s Nebula”) associated with it (Gyulbudagyan & Magakyan 1977, see WFPC2 image in Figure 1) is variable on the time scale of months (Cohen, Kuhl, Spinrad, & Harlan 1981). While extensive observations of PV Ceph and its outflow are available in the literature<sup>1</sup>, there are, to the best of our

---

<sup>1</sup>Arce & Goodman 2002a provides a lengthy introduction to this source, which we will not repeat here.

knowledge, no prior measurements of the source’s proper motion, or claims, as we make below, that it is moving unusually fast.

Analysis of PV Ceph’s environs leads us to believe that PV Ceph was ejected from the young cluster NGC 7023. We close this paper with a brief discussion, based on both theoretical and observational results, of how many young stars may be “speeding” far from their ancestral homes.

## 2. Evidence for Source Motion

In United States courts, the “beyond a reasonable doubt” standard is used in criminal cases, but for civil disputes, another standard, known as “preponderance of evidence” sets the bar. We should state at the outset that we can convict PV Ceph of speeding (at roughly  $20 \text{ km s}^{-1}$ ) on a “preponderance” of circumstantial evidence. However, as there are no direct proper motion measurements of PV Ceph<sup>2</sup> we cannot in good conscience offer a conviction “beyond a reasonable doubt.” Below, we will go into detail on the following three pieces of damning evidence, listed here in rough order of decreasing importance:

- Observed positions of HH knots on parsec scales are better explained in a scenario where PV Ceph is moving at a constant velocity (of  $\sim 20 \text{ km s}^{-1}$ ) than they are by hypothesizing angular separations of jet and counterjet of an angle other than  $180^\circ$  or by allowing for unpaired knots.
- Redshifted molecular gas appears to “trail” behind PV Ceph to the East, in addition

---

<sup>2</sup>We have placed an upper limit on the motion of PV Ceph by comparing the Palomar Plates with the Digital Sky Survey (which gives a time baseline of about 43 yrs). That limit, discussed further in section 4.1, is  $33 \text{ km s}^{-1}$ , in the plane-of-the-sky.

to forming a jet along the HH flow.

- Modeling the tilted “wobble” of the southern jet-like molecular outflow implies source motion, at  $\sim 20 \text{ km s}^{-1}$ , if the current outflow axis is nearly N-S, as implied by HST images.

Below, we explain this evidence, and then discuss the plausibility and implications of PV Ceph, and possibly other young stars, speeding through the ISM at velocities  $\sim 20 \text{ km s}^{-1}$ .

### 2.1. Geometry of the Knots in the HH flow

We were first alerted to the possibility of a high “peculiar” velocity for PV Ceph when we were trying to understand the relation between its optically detected giant Herbig-Haro flow (Reipurth, Bally, & Devine 1997) and the properties of its molecular outflow (Arce & Goodman 2002a,b, hereafter AGa and AGb, respectively). In trying to create “pairs” amongst the HH knots in the PV Ceph flow (see Figure 1), we initially saw two possibilities. First, we tried drawing straight lines *through* PV Ceph and finding paired HH knots along those lines on either side of the star. Attempting that, we noticed that several knots would be without partners on the opposite side of the source. No obvious explanations (e.g. high extinction) for the missing knots were very relevant. Second, we tried to find pairs of knots at similar distances from the source, the method of pairing one might expect from a flow emitting “ballistic” knots. Doing this, we noticed that lines drawn between pairs of knots at very similar distances did not all pass through the source. Instead, the halfway (a.k.a. bisector) point only passed through the source for the innermost pair of knots, and the halfway points for progressively more distant knots seemed to be moving along a line to the East (see Figure 1). The simplest explanation for this motion of the bisection points is that the outermost HH knot pair is oldest, and that the source has been moving, at roughly 20

km s<sup>-1</sup> (see below) to the West, at least since the initial ejection.<sup>3</sup> In the moving-source scenario we favor, the position angle of the flow is also changing, appearing to approach a N-S direction in a counter-clockwise direction (see Table 1).

### 2.1.1. *The Plasmon Model*

Imagine that a star moves in a straight line and periodically emits blobs of high-velocity gas that lead to HH knots. Assuming that the star’s motion is very slow compared with the initial knot (jet) speed, the key factor determining the path of a knot once it is emitted from the moving star is how quickly it decelerates in the ambient medium.<sup>4</sup> In the limit of no deceleration (a zero-density ambient medium), the component of a knot’s velocity along the star’s direction of motion will equal that of the star. So, even as a pair of knots moves outward from the star, the bisector of a line between them will never be seen to “lag” behind the star. In other words, with no deceleration by an ambient medium, one could never tell that the source of an HH-flow was moving from the knot pattern, because everything would apparently take place in a rest frame defined by the star. In the opposite limit of a very high-pressure ambient medium, a knot will rapidly lose the component of its velocity created by the star’s motion: as it moves outward in the “jet” direction, it will lag behind the source by an amount roughly proportional to the distance moved “outward” by

---

<sup>3</sup>An alternative explanation is that every jet emitted from (an almost-stationary) star bent in such a way as to give the current distribution of HH knots, where each pair is then separated by an angle significantly  $\neq 180^\circ$ . We consider this explanation too much of a conspiracy to be plausible.

<sup>4</sup>We are very grateful to James Yorke for asking a question which caused us to fully appreciate this point.

the knot scaled by the ratio of star-to-knot velocity (see below).<sup>5</sup>

For giant HH flows, on pc scales, the velocities, pressures and densities involved are such that neither the “zero-density” ambient medium (ballistic) or the “very rapid deceleration” picture typically applies. Instead, the deceleration history of the knots is critical to the geometry observed.

In 2000, Cabrit & Raga successfully modeled knot deceleration in the HH 34 “superjet” by assuming the source to be stationary and using what is conventionally known as a “plasmon” model (first studied analytically by De Young & Axford 1967; see also Cantó et al. 1998). In their Figure 1, Cabrit & Raga show that a plasmon model where clumps are decelerated simply by their interaction with a uniform density medium produces an excellent fit to the observed knot velocities in HH 34.

In this paper, we modify the plasmon model used by Cabrit & Raga (2000, in turn based on Cantó et al. 1998), to calculate the position of HH knots in a flow from a *moving* source, as a function of time. To do this, we treat each knot as a blob of gas, decelerating as it travels through an ambient medium, and we assume that blobs are ejected episodically, in diametrically-opposed pairs, from a source moving at constant velocity.

To model the knots in the PV Ceph flow as a set of decelerating “plasmon” blobs created by an episodic jet, we use the following generalizable procedure. Assume that a jet

---

<sup>5</sup>It is interesting to realize here that a model of a source moving through a medium at rest is quite equivalent to that of a stationary source in a moving medium. We thank the referee for pointing us to the elegant work on “HH jets in supersonic sidewinds” by Cantó & Raga (1995), Lim & Raga (1998) and Masciadri & Raga(2001). The estimates of PV Ceph’s velocity one can make using the formalism in Cantó & Raga (1995) is in line with the model we offer here.

is emitted in a direction defined in space by  $\hat{v}_j$ , from a source which is moving in a straight line defined by the direction  $\hat{v}_*$ . These two directions define the  $v_j - v_*$ , or the “jet-source motion,” plane, and the angle between them is  $\theta_o$ . The path of the knots in the  $v_j - v_*$  plane is then readily modeled by numerically integrating

$$\vec{v}(t) = \int \frac{d\vec{v}}{dt} dt + \vec{v}_j + \vec{v}_*. \quad (1)$$

where the deceleration of the plasmon,  $d\vec{v}/dt$ , is calculated using eq. 2, below. To compare this model with observations, one can either re-calculate the motion as projected from the  $v_j - v_*$  plane to the plane-of-the-sky frame, or de-project the observed positions and velocities into the more natural  $v_j - v_*$  plane itself. We choose to do the latter, as our model is then more intuitively understandable.

For a hypersonic, isothermal clump decelerated only by the gas drag of the ambient medium, the instantaneous deceleration can be written:

$$\frac{dv}{dt} = - \left( \frac{\xi \rho_{amb} c^4}{M} \right)^{1/3} v^{2/3}, \quad (2)$$

where  $v$  is the clump velocity at any instant,  $c$  is (traditionally) the isothermal sound speed,  $M$  is the constant mass of the clump,  $\rho_{amb}$  is the mass density of the ambient medium, and  $\xi = 14$  is a constant describing the shape of the plasmon (adopted from Cantó et al. 1998). For our purposes, we take  $c$  to be the typical line width in the ambient medium, since that describes the true ambient pressure, which far exceeds the isothermal sound speed.

While the instantaneous value of  $dv/dt$  is itself a scalar, we use  $d\vec{v}/dt$  in eq. 1 to mean the deceleration along the direction of the jet at a given time,  $t$ . In the numerical integration described above, we update the direction of  $\vec{v}$  for each time step in the calculation. This kind of numerical directional updating is obviously unnecessary for a stationary source, where the velocity of the plasmon changes only in magnitude, and not in direction<sup>6</sup>. In

---

<sup>6</sup>In a reference frame fixed to the sky, the path of each knot in a knot pair is a straight

that stationary-source case, the velocity of the knot as a function of radius can be written analytically, as

$$\frac{v_{knot}(r)}{v_j} = \left(1 - \frac{r}{d_o}\right)^{3/4} \quad (3)$$

$$d_o = \frac{3}{4} \left(\frac{Mv_j^4}{\xi\rho_{amb}c^4}\right), \quad (4)$$

where  $r$  is measured along the star-knot direction (Cantó et al. 1998, Cabrit & Raga 2000).

Unlike the situation in HH34 where Cabrit & Raga could fit their plasmon model to detailed observations of knot velocities, there is no extensive set of velocity measurements for the PV Ceph flow. Instead, David Devine’s Ph.D. thesis gives radial velocity measurements of for just three knots:<sup>7</sup>  $v_{radial} \sim -271$  km s<sup>-1</sup> for HH215A, and  $v_{radial} \sim -55$  and 52 km s<sup>-1</sup> for HH315B and HH315E, respectively (Devine 1997). What we *do* have in PV Ceph are detailed measurements of current knot *positions* (Table 1), and very good observational estimates of the ambient velocity dispersion and density (Table 2). We only require that our moving-source plasmon model fit the observed knot *positions* (Figure 2). We use the few velocity measurements available as a way to: 1) estimate a velocity for PV Ceph’s jet very close to the source; and 2) check that the velocities predicted by our model for knots farther from the source are reasonable.

To estimate the jet velocity close to the source, we conservatively assume an inclination

---

line (see Figure 7). It is only in a frame tied to the source that a knot’s path appears to curve. Figure 2, discussed later in this section, shows the locus of all knot positions in a jet-source plane where the jet direction is fixed and (0,0) corresponds to the source position.

<sup>7</sup>Note that due to historical (and nomenclature) reasons, the “PV Ceph” flow is comprised of two sets of HH objects, with different numbers. “HH 215” refers only to the jet very close to the source, and “HH 315” includes all the knot pairs we are modeling here. See Figure 1 for a finding chart.

angle of the HH 215 flow of  $45^\circ$  (as in Devine 1997). The measured radial velocity for HH215A then implies that the initial 3D velocity of “a” jet from PV Ceph is of order nearly  $400 \text{ km s}^{-1}$ . The same  $45^\circ$  inclination angle implies that our plasmon model should predict velocities of order  $100 \text{ km s}^{-1}$  for the “middle” pair of knots (B-E) in the HH315 flow. Keep in mind, however, that there is no reason to assume that the initial ejection speed—or the inclination angle—of the jet(s) that created each pair of knots in the PV Ceph flow was the same—this is only a simplifying assumption in our “fitting” of a plasmon model. In reality, it is likely that the jet is episodic, emitting bursts of varying strength (Arce & Goodman 2001), and that its inclination angle varies—especially given that we know its position angle on the plane of the sky varies. Nonetheless, in order to make a simple model of knot deceleration, we ignore the second-order effects that variability in ejection velocity or  $\theta_o$  have on the plasmon calculation.

The dark curve (labeled “ $22 \text{ km s}^{-1}$ ”) in Figure 2<sup>8</sup> shows the locus of possible knot positions in the  $v_j - v_*$  plane for the moving-source plasmon model outlined above, under the physical conditions listed in Table 2. Exactly where knots lie along this curve depends only on when they were emitted. To facilitate data-model comparison, the three black filled circles show positions corresponding to the PV Ceph knots—if the change in jet ejection angle with time is ignored<sup>9</sup>. As the figure shows, the observed knot positions in the PV Ceph flow are remarkably well-fit by a simple  $22 \text{ km s}^{-1}$  plasmon model. The two lighter curves in Figure 2 show how sensitive the model is to assumptions about the velocity of the central source. As expected, for a source velocity very slow ( $v_* = 1 \text{ km s}^{-1}$ ) compared with the jet velocity ( $v_j = 350 \text{ km s}^{-1}$ ), the knots would not be seen to lag behind the star at

---

<sup>8</sup>The (0,0) of the coordinate system in Figure 2 is tied to the position of PV Ceph.

<sup>9</sup>Figure 7 shows an illustration of what the same ( $22 \text{ km s}^{-1}$ ) model shown in Figure 2 gives when the jet angles are purposely adjusted to match those listed in Table 1.

all, whereas for a speeding source ( $v_* = 100 \text{ km s}^{-1}$ ), the knots would be seen to lag almost immediately.

### 2.1.2. Assumptions and Uncertainties in the Plasmon Model

While the “22 km s<sup>-1</sup>” source velocity curve shown in Figure 2 and parameterized in Table 2 clearly gives a very good fit to the PV Ceph flow’s knot positions, we are *not* claiming that 22 km s<sup>-1</sup> is the “exact” velocity of the source. Instead, after an extensive search of parameter space in our plasmon model, we find the set of parameters listed in Table 2 to come closest to fitting our data.

We accomplish the seemingly impossible trick of fitting six data points (two-dimensional positions for 3 pair of knots) with a model that requires nine inputs by constraining many of the inputs with additional observations. As shown in Table 2, the density and velocity dispersion in the calculated plasmon model are tied to observations of PV Ceph’s host cloud in <sup>12</sup>CO and <sup>13</sup>CO (AGa). The angle between  $\hat{v}_j$  and  $\hat{v}_*$  is taken to be 90° because the current  $\hat{v}_j$  is clearly N-S (see WFPC2 image in Figure 1) and  $\hat{v}_*$  appears to be from E to W based on the geometry shown in Figure 1. The inclination angle of the flow to the sky is assumed to be 45°, as a conservative guess<sup>10</sup>, and the inclination angle of the star’s motion w.r.t. the plane-of-the sky is assumed to be 20°, since any much larger angle would not give PV Ceph sufficient plane-of-the-sky motion for us to have noticed it. The mass

---

<sup>10</sup>Gómez, Kenyon, & Whitney (1997) model the HH 315 flow as emanating from a stationary precessing source, and derive an inclination angle of just 10° to the plane of the sky. Since our current analysis strongly suggests that the HH knot positions in the flow are critically effected by source motion (and are not as well-modeled as arising from a stationary precessing source) we do not adopt the 10° inclination angle the Gómez et al. model implies.

of each ejected blob,  $3 \times 10^{-4} M_{\odot}$ , and the geometric factor describing the shape of the plasmon,  $\xi = 14$ , are assumed to be similar to the values Cabrit & Raga found for HH 34. So, with those seven parameters held fixed at the values shown in Table 2, we can “fit” the positions of the HH knots in the PV Ceph flow by *only adjusting the star and initial jet velocities*. If we use the radial velocity for HH 215A measured by Devine (see above) to set  $v_j \approx 350$  to  $400 \text{ km s}^{-1}$ , we find  $v_* \approx 22 \text{ km s}^{-1}$  as a “best fit.”

After stretching each of the input parameters to within what seem reasonable bounds based both on our observing experience and on where they cause the plasmon model to grossly fail, we are willing to predict, that the “true” three-dimensional velocity of PV Ceph is more than 10 but less than  $40 \text{ km s}^{-1}$ .

### 2.1.3. Utility of Plasmon Models in the Real ISM

In reality, the velocity and mass of each knot emitted in a giant HH flow is surely not the same (Arce & Goodman 2001), and the density and velocity dispersion into which the knots travel is not uniform. Thus, despite what may appear as exquisite model-data agreement in Figure 2, the plasmon model should not be taken as more than a 1st-order estimate of the interaction of HH knots and the ambient ISM.

In the lower panel of Figure 3, we show knot velocity as a function of distance from the source, for the “ $22 \text{ km s}^{-1}$ ” moving-source plasmon model. Grey circles are plotted —on the calculated curves— at the deprojected distances of the observed knot pairs. As mentioned above, in the HH 315 flow, Devine (1997) measured radial velocities only for knots B and E, both of which deproject to about  $75 \text{ km s}^{-1}$ , assuming a  $45^\circ$  inclination angle for the flow. The strict plasmon model shown in Figure 3 would predict twice that velocity for the B-E knot pair. Does this mean our model is wrong? No —it could well mean that ignoring

changes in jet ejection angle in PV Ceph would not be a good assumption in a more detailed model. If the jet giving the B-E knot pair is more along the line-of-sight than the others, then the knots with what seem “too low” velocities are in fact further from the source in 3D, as the model predicts for the observed radial velocities (see Figure 3). Alternatively, if the B-E jet is more in the plane-of-the sky than the others, Devine’s measurement of its radial velocity would need to be “deprojected” to 3D by a larger correction factor, again bringing it into line with the model.

Another explanation altogether for any detailed mismatches between model and data is simply that the velocities with which knot pairs are emitted in the PV Ceph flow is variable enough to explain the discrepancies. If we had detailed measurements of the radial velocities and proper motions of all of the knots in PV Ceph, we could construct a much more sophisticated model of the flow’s history and geometry. The plasmon ideas explored here will lie at the heart of future more sophisticated models, and as such, they are very useful.

Figure 3 also makes another important point —about the age of outflows. The top panel of Figure 3 shows that if knots slow down at the rate implied by the plasmon model, then estimating the age of an outflow by dividing the distance of the outermost knot by the knot’s observed speed (i.e. calculating a dynamical time) will significantly overestimate the age of the flow. The plasmon model of PV Ceph’s flow implies that the slowest currently-supersonic blob (velocity marginally greater than the ambient dispersion of  $3.2 \text{ km s}^{-1}$ ) would have left PV Ceph 10,000 years ago. For comparison, the dynamical age of PV Ceph implied for a knot moving at this minimum speed ( $3.2 \text{ km s}^{-1}$ ) would be 560,000 years! In reality, velocities of several tens of  $\text{km s}^{-1}$  are required to produce shocked gas visible optically, and the dynamical time of the “outermost” knots in a giant Herbig-Haro flow are likely to overestimate the age of the flow by about an order of magnitude (see

Figure 3).

The bottom panel of Figure 3 shows that blobs will slow to velocities  $< 10 \text{ km s}^{-1}$  at  $\sim 2 \text{ pc}$  in the PV Ceph flow, and this slowdown—which limits the observable size of a flow—will happen at some similar radius in other flows as well.<sup>11</sup>

Thus, taking the results of the two panels of Figure 3 together, we see that the “size” of an outflow we see now is determined only by how far the oldest knot *we can still see as moving and shocked* has traveled in to the ISM, and estimating the age of the flow based on the parameters of this knot is a flawed procedure. The flow’s age will be overestimated by the dynamical time of the outermost knot—and, perhaps worse, the age will be underestimated by assuming that outermost knots we see date the flow’s birth. Older, unseen, knot pairs may have blended back into the ISM by now. Thus, the plasmon analysis leaves us realizing that many outflow “ages” estimated in the extant literature may be incorrect.

## 2.2. A Trail of Redshifted Gas

Position-velocity diagrams of  $^{12}\text{CO}$  (2-1) and  $^{13}\text{CO}$ (1-0) emission each show a very peculiar extension to highly-redshifted velocities right at the position of PV Ceph (see Figure 15 of AGb, and Figure 4 of AGa, respectively). If PV Ceph is indeed zooming through the ISM with a velocity near  $20 \text{ km s}^{-1}$ , then the moving blob of gas gravitationally bound to PV Ceph is likely to leave a trail of accelerated gas in its wake. The trail might

---

<sup>11</sup>In the two HH flows where direct proper motion and radial velocity measurements are both available [HH34 (Devine, Bally, Reipurth, & Heathcote 1997), discussed in §2.1.1, and HH7-11 (Noriega-Crespo & Garnavich 2001)] the data show decreasing knot velocity with source distance.

be created in one of two ways. First, one could expect gas to be “swept-up” by the action of the dense, supersonic, blob in much the same way it is in the “prompt-entrainment” picture of jet-driven outflow. Alternatively, if the pressure drop created in space after the moving blob has passed-through is great enough, molecular gas clouds could condense out of lower-density warmer ambient material. This second way to form a trail is analogous to the formation of “vapor” or “con” trails behind airplane wings.

In the two short sections below, we first discuss the observations of the trail of mildly redshifted molecular gas (2.2.1) created by PV Ceph’s motion, and then consider how much gas is likely to be bound to PV Ceph (2.2.2). In this paper, we do not consider in detail whether the swept-up trail or “con-trail” scenario is more likely, but we suggest this as an interesting question for future work.

### *2.2.1. Trail in the $100 \text{ cm}^{-3}$ Molecular Gas*

Detailed mapping of the  $^{12}\text{CO}$  (2-1) emission, which traces densities  $\sim 100 \text{ cm}^{-3}$ , around PV Ceph has revealed a “trail” in the mildly redshifted gas distribution in exactly the direction PV Ceph would have come from in the model described in §2.1.

The contour map labeled “more redshifted” in Figure 1 shows  $^{12}\text{CO}$  (2-1) emission integrated from 4.15 to 6.46  $\text{km s}^{-1}$  (based on Figure 6 of AGb). This highly redshifted molecular gas is associated with the current jet emanating from PV Ceph, whose plane-of-the-sky orientation (like the optical flow in the Figure 1 panel labeled “WFPC2”) is almost exactly N-S (§2.3). The “ambient”  $^{12}\text{CO}$  (2-1) LSR velocity near PV Ceph is  $\sim 2.5 \text{ km s}^{-1}$  (AGa). The panel labeled “less redshifted” in Figure 1 shows  $^{12}\text{CO}$  (2-1) emission integrated from 3.16 to 4.15  $\text{km s}^{-1}$  (based on Figure 6 of AGb), and it shows two important features. First, the jet itself is obviously still present, although its orientation, especially near the tip,

curves back toward the East. That curvature is consistent both with our proposed general clockwise rotation of the jet direction over time, and/or with motion of the source from East to West. (Slower material is older in the decelerating-jet-from-a-moving-source picture and would lie to the East of the faster material.) Second, and more importantly, the “less redshifted” map shows a *trail* in the molecular gas, extending all the way to the edge of this map, in exactly the direction PV Ceph would have come from in the moving source model. In fact, the same kind of extension is evident on larger scales. The pc-scale (main) image of the outflow in Figure 1 also clearly shows an extension of redshifted emission toward the East. For readers unfamiliar with outflow maps, note that this kind of asymmetry is *not* common in these maps.

We propose that the “redshifted” trail of emission seen in  $^{12}\text{CO}$  (2-1) to the East of PV Ceph is caused by the interaction of the ambient medium with a gravitationally bound higher-density blob (see §2.2.2) traveling along with PV Ceph, moving E-W and away from us at an angle of  $\phi_{\text{star-sky}} = 20^\circ$  (see Table 2). Motion away from us would redshift the “trailing” material with respect to the cloud velocity. If we assume that the full E-W stretch of the redshifted material in the main panel of Figure 1 (at the declination of PV Ceph) is due to gas created by this interaction, PV Ceph would now have travelled at least 0.2 pc. At  $20 \text{ km s}^{-1}$ , traveling 0.2 pc takes 10,000 years, which is then a lower limit on the age of PV Ceph.

### 2.2.2. Dense Gas Moving With PV Ceph

The upper left panel of Figure 1 shows a map of  $^{13}\text{CO}$  emission between 3.15 and 3.71  $\text{km s}^{-1}$  near PV Ceph (from AGB, Figure 7). In other words, this is a map of  $\sim 1000 \text{ cm}^{-3}$  gas moving with an average velocity redshifted by about  $1 \text{ km s}^{-1}$  with respect to the ambient material in the vicinity of PV Ceph. Since the gas traced by  $^{13}\text{CO}$  is only  $\sim 10\times$

denser than that traced by  $^{12}\text{CO}$  (2-1), we expect that most of the redshifted  $^{13}\text{CO}$  evident in the upper left panel of Figure 1 was moved to these velocities by the same mechanism that redshifted the  $^{12}\text{CO}$  discussed above in §2.2.1. It is possible, though, that  $^{13}\text{CO}$  is a high-enough density tracer that we could detect a *small* clump gravitationally bound to PV Ceph moving along with it. The size of that clump depends on a competition between gravity, which acts instantaneously to draw material into a blob around a point source, and gas drag, which tries to keep material where it was, but can only do so at a speed governed by the pressure of the gas.

To illustrate how much gaseous material might move along with a speeding protostar, Figure 4 shows the modified “Bondi-Hoyle” accretion radius for a point mass moving through an ambient medium (see Bonnell et al. 2001),

$$R_{BH} = \frac{2GM_*}{\sigma^2 + v_{rel}^2} = \frac{GM_*}{\sigma_{eff}^2}, \quad (5)$$

where  $v_{rel}$  is the dimensionally-averaged speed with which the point mass ( $M_*$ ) moves through the ambient medium whose one-dimensional velocity dispersion is  $\sigma$ . For PV Ceph, using Bonnell et al.’s formalism,  $v_{rel} = 7.3 \text{ km s}^{-1}$ , the average of 22, 0, and 0  $\text{km s}^{-1}$ . The velocity dispersion around PV Ceph is much less than this, so we can ignore the  $\sigma^2$  term in eq. 5, making  $\sigma_{eff} \approx v_{rel}/\sqrt{2} \approx 5.2 \text{ km s}^{-1}$ . The mass of PV Ceph is not precisely known, but is likely to be  $< 7 M_\odot$  (less than the most massive Ae/Be stars). So, examining Figure 4 for the conditions relevant to PV Ceph, we see that a bound “clump” moving along with a  $7 M_\odot$  star would have a diameter of  $< 0.001 \text{ pc}$ , or about 0.5 arcsec at 500 pc. Thus, even the highest-resolution molecular-line observations shown in Figure 1 ( $^{13}\text{CO}$  map at the upper left) could not spatially resolve the “Bondi-Hoyle” clump that would be speeding along at  $\sim 22 \text{ km s}^{-1}$  with PV Ceph.

In our FCRAO observations of PV Ceph, published in AGa, we also searched for  $\text{N}_2\text{H}^+$  emission associated with the star. Ordinarily,  $\text{N}_2\text{H}^+$  would reveal a  $> 10^4 \text{ cm}^{-3}$  “dense

core” associated with such a powerful outflow source. Curiously, no  $\text{N}_2\text{H}^+$  emission was detected. We suspect that PV Ceph’s rapid motion, which would make a bound core very small (see Figure 4) is responsible for this state of affairs, and we discuss how a star might have an outflow with no dense core in §4.3.

In principle, Bondi-Hoyle accretion is not the complete mechanism determining how big a blob would *appear* to surround a rapidly-moving young star. While it is true that PV Ceph itself can only carry along a small ( $\sim 0.001$  pc) blob, that very dense blob will in turn drag less dense gas along with it, at a lower speed. The asymptotic evolution of this process creates the appearance of a larger blob when observed at a density lower than that of the clump “bound” to PV Ceph. The gas physics associated with this process are not dissimilar to those of the plasmon problem discussed in §2.1.1, but have not, to our knowledge, been exactly worked out for the specific case of a gravitating point-mass+cocoon moving through a relatively high-pressure medium. Thus, we conclude this section with the suggestion that the morphology of the mildly-redshifted  $^{13}\text{CO}$  emission around PV Ceph might be well-explained by a detailed gas-dynamical model of a point-source plus it’s gravitationally-bound/swept-up cocoon moving through a molecular cloud.

### 2.3. Tilted Wiggle in the Innermost Jet

The wiggles in the jet of “more-redshifted” gas shown in the lower right corner of Figure 1 (see AGb, Figure 18, for detail) are well fit by a model where they arise from a precessing jet, the source of which is moving at roughly  $20 \text{ km s}^{-1}$ .

The inset HST WFPC2 image (Padgett et al. 1999, and Padgett, personal communication) of the inner region of the PV Ceph outflow shown in Figure 1 shows the current symmetry axis of the PV Ceph biconical nebula to be very close to N-S. Thus, we

take a position angle of zero degrees, shown as a yellow line in the lower panels of Figure 1, to be the orientation of the jet coming from PV Ceph “now”. This orientation is consistent with the counter-clockwise rotation of PV Ceph’s flow implied by the arrangement of large-scale HH knots (see Figure 1 and Table 1), and with the analysis of the redshifted molecular jet presented in §2.2.1.

Figure 5 shows the Right Ascension (column number) of the peak emission in the “more redshifted”  $^{12}\text{CO}$  (2-1) gas (shown in the lower-right panel) as a function of declination (row number; see AGb, Figure 18). An excellent fit to these data is obtained by modeling them as the sum of a constant source motion (shown here as the sloping line in the left panel Figure 5) plus a precession of the jet (sine wave shown in the right panel of Figure 5).

As we stated in §2.1.1, in the limit of a very high-pressure ambient medium, a knot will rapidly lose the component of its velocity created by the star’s motion: as it moves outward in the “jet” direction, it will lag behind the source by roughly the distance moved outward by the knot times the ratio of star-to-knot velocity. This “high-pressure” limit is relevant to the redshifted CO jet-like lobe modeled in Figure 5 (since it lies in a high-density region), so the slope of the linear fit shown in the left panel implies that

$$v_* = 0.06 \times v_{jet}. \quad (6)$$

For the *same*  $350 \text{ km s}^{-1}$  jet velocity assumed in §2.1.1 (see Table 2), equation 6 gives  $v_* = 21 \text{ km s}^{-1}$  —in astonishingly good agreement with the independently-derived source velocity based on the plasmon model!<sup>12</sup>

If instead of assuming that the jet is now perfectly N-S, we instead assume an orientation more toward the overall tilt of the apparent  $^{12}\text{CO}$  (2-1) jet, the source velocity

---

<sup>12</sup>Possible origins of the precession implied by the sinusoidal variations are discussed in detail in AGb.

is reduced. But, keep in mind that the HST image essentially rules out that the current jet direction is the one given by even the most redshifted  $^{12}\text{CO}$  (2-1) gas (Figure 1, bottom-right panel). Alternatively, if we increase our estimate of the jet velocity then the source velocity will increase. The key point remains, though, that for the most reasonable assumptions, of a N-S current jet orientation, and a  $350 \text{ km s}^{-1}$  jet velocity, our modeling of the wiggles in the south jet-like redshifted lobe implies the *same*  $\sim 20 \text{ km s}^{-1}$  velocity for *PV Ceph* as the plasmon model of the larger scale (HH 315) flow.

### 3. Possible Causes of “Speeding”

If *PV Ceph* really is moving at  $\sim 20 \text{ km s}^{-1}$ , how did it get such a high velocity? Below we consider several hypothetical scenarios, in order of decreasing *a priori* likelihood.

#### 3.1. Runaway star from a young stellar cluster

The nearest (known) stellar cluster to *PV Ceph* is NGC 7023, a cluster with a stellar mass of roughly  $100 M_{\odot}$  (Aveni & Hunter 1969) whose most massive member is the B3e star HD200775 with mass  $10 M_{\odot}$  (Mendoza 1958; Strom et al. 1972; Elmegreen & Elmegreen 1978). Figure 6, which includes a large-scale  $100 \mu\text{m}$  IRAS image, shows NGC 7023 to lie in *exactly* the direction *PV Ceph* would have come from according to our analysis in §2 (see also Figure 1). The LSR velocities of the molecular gas associated with NGC 7023 are primarily between  $2$  and  $3 \text{ km s}^{-1}$ , as is the case for *PV Ceph* (Gerin et al. 1998). The Hipparcos distance to NGC 7023 is about  $430 \text{ pc}$  (Perryman et al. 1997). If *PV Ceph* is at the same distance (which is consistent with uncertainties), then it is currently about  $10 \text{ pc}$  away from the center of NGC 7023.

We emphasize that the long arrow shown in Figure 6<sup>13</sup> is just the extension of the short line segment shown as the path of PV Ceph in Figure 1. We were very surprised to find that path pointing straight at NGC 7023. The probability of the position angle of PV Ceph’s path on the plane of the sky accidentally matching a PV Ceph-NGC 7023 connector to better than a few degrees is only about 1 percent ( $3^\circ/360^\circ$ ). Combining the similar distances of NGC 7023 and PV Ceph with the low probability of randomly finding the “right” plane-of-the-sky orientation for PV Ceph’s path, we know that at least three of the four space-time dimensions strongly imply that PV Ceph came from NGC 7023.

What about the time dimension? At its current velocity of  $\sim 20 \text{ km s}^{-1}$  it would have taken PV Ceph  $\sim 5 \times 10^5 \text{ yr}$  to reach its current position. This amount of time is approximately equal to or greater than the estimated age of PV Ceph—which is thought to be a Class I protostar of spectral type A5 with an age  $\sim 10^5 \text{ yr}$  (Fuente et al. 1998)<sup>14</sup>. On the other hand, if PV Ceph came from NGC 7023, its *initial* velocity could have been larger.<sup>15</sup> Without knowing where in the gravitational potential of the cluster PV Ceph might have originated, it is very difficult to estimate its potential initial speed, but it is reasonable to guess  $> 20 \text{ km s}^{-1}$ . For reference, to acquire a velocity of  $22 \text{ km s}^{-1}$  by converting gravitational to kinetic energy in a “slingshot” encounter with a star of mass  $M_{scat}$  requires a closest approach of  $R_c[\text{A.U.}] = 4.5M_{scat}/M_\odot$  (e.g. 45 A.U. for a  $10 M_\odot$  star). N-body simulations of open star clusters show that dynamically ejected stars can reach velocities of up to  $200 \text{ km s}^{-1}$  (e.g., Leonard & Duncan 1990, see also de La Fuente

---

<sup>13</sup>The slight curvature of this arrow accounts for the map projection scheme, and in fact represents a straight-line path through space.

<sup>14</sup>This age estimate assumes a “normal” past for PV Ceph. If, in fact, it spent some large fraction of its life wandering at high speed across space, age estimates may need revision!

<sup>15</sup>We thank Laurent Loinard for inspiring us to consider this idea.

1997, and §3.2, below). If PV Ceph was in fact ejected at  $> 20 \text{ km s}^{-1}$ , NGC 7023’s gravity would not do much to slow the star and whatever disk or blob was bound to it, but the cumulative effect of all the matter (shown as green and yellow in the dust emission map in Figure 6) between NGC 7023 and PV Ceph’s current position could potentially have slowed it —through primarily drag forces— to  $20 \text{ km s}^{-1}$ . Thus, the  $\sim 5 \times 10^5 \text{ yr}$  to get from NGC 7023 to PV Ceph’s current position is an upper limit, and it is plausible that PV Ceph was born in NGC 7023.

The inset Sloan Digital Sky Survey Image of NGC 7023 in Figure 6 reveals a striking dark swath across the Southern part of the cluster. The Figure also shows that the  $174^\circ\text{E}$  of N path of PV Ceph implied by our analysis of its outflow (§2) would have it coming from a direction nearly perfectly aligned with this dark lane. It is surely tempting to think that PV Ceph’s ejection from NGC 7023 might have caused this “exit wound.” The lane is, presently, of order 0.1 pc wide. The ambient ( $^{13}\text{CO}$ -traced molecular) gas in NGC 7023 has a velocity dispersion  $\sim 1.5 \text{ km s}^{-1}$  (Ridge et al. 2003), which implies that closing the current gap by turbulent diffusion would take about  $8 \times 10^4$  years, that is 6 times less than the upper-limit for the time since PV Ceph’s ejection. Therefore, if the rift in NGC 7023 were in fact an exit wound caused by the escape of PV Ceph, then either the wound must have originally been much wider, the pressure in the rift was or is higher than ambient, or PV Ceph’s initial velocity was much higher than  $20 \text{ km s}^{-1}$ . If the rift was caused by the exit of PV Ceph from NGC 7023, and it is now half-closed, PV Ceph’s ejection would have been 133,000 years ago, and its time-averaged speed since ejection would be almost implausibly high — $75 \text{ km s}^{-1}$ . Alternatively, if PV Ceph left a shock-heated trail when it created the rift we see now, the rift would have had a velocity dispersion (and pressure) greater than ambient, and would have taken longer to close.

Existing maps of the distribution of molecular gas in NGC7023 bear on the importance

of the “rift” seen at optical and infrared<sup>16</sup> wavelengths in two ways. First, HD200775 (the 10  $M_{\odot}$  star that illuminates NGC7023) is centered in a bipolar cavity which is oriented roughly E-W (Watt, Burton, Choe, & Liszt 1986; Fuente, Martin-Pintado, Rodriguez-Franco, & Moriarty-Schieven 1998; Ridge et al. 2003), so that the apparent rift does lie within, or possibly near the edge of, the western side of the cavity. We note, though, that the opening angle of the cavity is much larger than that of the rift seen optically. Second, the integrated emission from  $^{12}\text{CO}$  in NGC7023 shows a very distinct hole (Elmegreen & Elmegreen 1978) in what appears to be the place where PV Ceph would have punched out of the cloud, if it indeed had traveled down the optical “rift” and out the far side of the cloud (see Elmegreen & Elmegreen 1978, Figure 1). The hole is too large ( $\sim 0.7$  pc) to have been punched by the ejection of just the star, but its existence is provocative nonetheless.

### 3.2. Ejection from a Multiple Star System

Numerical studies of the interactions of multiple star systems reveal that most systems with three or more members are unstable (Valtonen & Mikkola 1991; Kroupa 1998; Kiseleva, Colin, Dauphole, & Eggleton 1998). These studies show that within about 100 crossing times (or approximately a few times  $10^4$  yr) it is very probable that a member of the system will be ejected (see Reipurth 2000 for details). The ejected star will not always be the least massive member of the system. The velocity of the ejected member, as shown by the numerical simulations of Sterzik & Durisen (1995), is typically 3 to 4  $\text{km s}^{-1}$ , but can reach values of 20  $\text{km s}^{-1}$  and more. In fact, Kiseleva, Colin, Dauphole, & Eggleton (1998) find escape speeds in excess of 30  $\text{km s}^{-1}$  1 % of the time in systems with between 3 and

---

<sup>16</sup>2MASS and Spitzer Space Telescope (Megeath et al. 2004) infrared images also show a gap in emission from NGC7023 along the direction PV Ceph would have exited.

10 stars. The same simulations give velocities between 10 and 20 km s<sup>-1</sup> 20 to 30 % of the time and between 20 and 30 km s<sup>-1</sup> 3 to 5 % of the time, with the exact percentages depending on the group’s initial mass and velocity distributions. So, PV Ceph’s  $\sim 20$  km s<sup>-1</sup> velocity would not be considered extreme at all in the context of these simulations.

If PV Ceph obtained its current speed as a consequence of being ejected from a multiple star system —and that system were something smaller than NGC 7023— one would expect to find the remaining members of this stellar system “nearby.” The nearest detected sources (shown as white stars in Figure 6) which could be young stars are two faint IRAS point sources east of PV Ceph, IRAS 20495+6757 and IRAS 20514+6801, at 25.6’ and 37.4’ from PV Ceph, respectively (see IRAS point source catalog). Assuming that these two sources are at  $d \sim 500$  pc, then they are at distances of 3.7 pc and 5.4 pc from PV Ceph. At a velocity of about 20 km s<sup>-1</sup> it would have taken PV Ceph  $2 - 3 \times 10^5$  yr to travel from the current position of IRAS 20495+6757 and IRAS 20514+6801 to its current position. As was the case for the NGC 7023 ejection scenario, this time is a good fraction of the estimated age of PV Ceph. Even if the different members of the putative multiple system broke up half-way between the current position of PV Ceph and these IRAS sources, it would have taken PV Ceph about 100,000 years to reach its current position at a speed of 20 km s<sup>-1</sup>. And, again as in the NGC 7023 scenario, it is possible that the initial ejection speed of PV Ceph was  $> 20$  km s<sup>-1</sup>, reducing the travel time to its current location. Given that the back-track (shown in purple in Figure 6) of PV Ceph aligns so perfectly with NGC 7023, and not very well at all with either of these IRAS sources, we find it much more likely that PV Ceph was ejected from NGC 7023 (see §3.1) than from a smaller multiple system with either of these anonymous IRAS sources.

To be thorough, we mention that it is also possible that PV Ceph’s ex-companion(s) has(have) not yet been detected, and is(are) still close ( $\leq 5'$ ) to PV Ceph, and thus

unresolved by IRAS. Reipurth, Bally, & Devine (1997) speculate that HH 415, near the north-western edge of the optical nebula (see Figure 1) is formed by another (yet undetected) young star in the region. So, while it is not impossible that the source of HH 415 is PV Ceph ex-companion, this seems much less likely than the NGC 7023 scenario.

### 3.3. Random Motions

Lastly, it is not crazy to think that PV Ceph’s  $\sim 20 \text{ km s}^{-1}$  speed might be due to purely random motions. Proper motion studies of groups of associated stars from the same star-forming region show that the three-dimensional velocity distribution of the studied samples have a  $1\text{-}\sigma$  dispersion about 3 to 7  $\text{km s}^{-1}$  (e.g., Jones & Herbig 1979; Frink et al. 1997; Sartori et al. 2003). Thus, even though the frequency of stars with velocities near  $20 \text{ km s}^{-1}$  (i.e., about a 3 to 5- $\sigma$  deviation from the mean) is very low, it is still a non-zero quantity. PV Ceph could simply be one of the few stars in the high-velocity tail of the velocity distribution of young stars. Finding such an outlier would not be unlikely, since the telltale signs of motion discussed in §2 would be more apparent in a source moving unusually fast. Again, though, we find this possibility less attractive than the NGC 7023 idea.

## 4. Implications of High Velocity in Young Stars: Admitting a More Dynamic Star-Forming ISM

### 4.1. How Common is Speeding?

Amongst massive main-sequence stars, speeding is a relatively common, and oft-documented, offense (e.g. Stone 1991). Thanks to a plethora of proper motion measurements from Hipparcos, it has become clear that both a supernova ejection mechanism (where

a star is shot out when its companion explodes; Blaauw 1961) and a binary-binary collision mechanism (where two binary systems collide and one star is scattered off through many-body interactions (e.g. Clarke & Pringle 1992)) can produce so-called “runaway” O and B stars, whose velocities can exceed  $100 \text{ km s}^{-1}$  (Gies & Bolton 1986; Hoogerwerf, de Bruijne, & de Zeeuw 2001).

Amongst young and forming stars, the propensity for speeding is mostly theoretical. Many simulations, of cluster (e.g. Leonard & Duncan 1990; Bate, Bonnell, & Bromm 2002, 2003; Bonnell, Bate, & Vine 2003), small multiple (e.g. Sterzik & Durisen 1995; Kiseleva, Colin, Dauphole, & Eggleton 1998), and interacting binary (e.g. Kroupa 1998) systems, show that large numbers of stars should be ejected during the star formation process. However, most very young stars are active, heavily embedded and/or associated with copious and variable nebulosity, making radial velocity or proper motions measurements challenging to impossible.

Nonetheless, PV Ceph is not the only young star to have been observed speeding —a handful of other young stars have also been justifiably accused (if not certainly convicted) of going very fast. Plambeck et al. (1995) show that the Becklin-Neugebauer object (BN) and the radio source “I” in the Orion KL nebula are moving apart at  $\sim 50 \text{ km s}^{-1}$ . From their data it is not certain if one or both objects are moving. However they suggest that BN is the more likely candidate, and that it is probably a runaway star that formed in the Trapezium cluster. The proper motion study of Loinard (2002), using two epochs of VLA 3.6-cm continuum data, suggests that component A1 in the IRAS 16293-2422 protostellar system could be a high-speed protostar with a velocity of  $\sim 30 \text{ km s}^{-1}$ . The multi-epoch study of Loinard, Rodríguez, & Rodríguez (2003) proposed that a member of the T Tau triple system has recently been ejected and is now moving at  $\sim 20 \text{ km s}^{-1}$ . But, the recent work of Furlan et al. (2003) shows that the radio-IR association made to reach this

conclusion was likely in error, so we do not count this as a case of speeding. In their study of proper motions of T Tauri variables in the Taurus-Auriga complex, Jones & Herbig (1979) reported that RW Aur has a velocity of  $\sim 16 \text{ km s}^{-1}$  on the plane of the sky. We do not count this claim of speeding either, because more recent proper motion measurements of this star by the Hipparcos and Tycho 2 missions show that the original measurements by Jones & Herbig (1979) are likely incorrect, and that the proper motion of RW Aur is within the typical  $2 \text{ km s}^{-1}$  velocity dispersion of the cloud (L. W. Hartmann 2004, private communication). In cases more similar to PV Ceph’s, where jet geometry is suggestive, Bally, Devine, & Alten (1996) suggest that motion at  $5$  to  $10 \text{ km s}^{-1}$  might explain the swept-back shape of the giant HH flow from B5-IRS1 in Perseus. And, Bally & Reipurth (2001) report the discovery of three jets in NGC 1333 cluster with a C-shaped symmetry, similar to the B5-IRS1 outflow, with bending towards the cluster core. They argue that the most likely scenario that explains the particular shape of these jets is one in which the jet sources have been dynamical ejected from the cluster and now are moving at about  $10 \text{ km s}^{-1}$  through the medium<sup>17</sup>. Thus, at least seven young stars (PV Ceph, BN/Source I, IRAS 16293-2422 (A1), B5-IRS1, and three outflow sources in NGC 1333 (HH 334, HH 449, and HH 498)) have been accused at traveling at speeds in excess of  $10 \text{ km s}^{-1}$  through the interstellar medium.

Clearly, seven stars, all discovered to be speeders by serendipity, is not a sample with which one can do statistics, so it is hard to say just how globally common “speeding” is amongst young stars. Nonetheless, the fact that seven speeders were caught without

---

<sup>17</sup>The work of Bally et al. (1996) and Bally & Reipurth (2001) give only rough estimates of the stellar velocities: they do not employ a deceleration model like the one used here for PV Ceph. If such a model were applied in the case of B5-IRS1, the velocity derived would be significantly larger.

directed law-enforcement efforts surely suggests that a focused campaign to measure the velocities of young stars is now in order. This campaign will not be easy with existing data. To give an example, with a comparison of the original Palomar Survey (observed in 1952) and the Sloan Digital Sky Survey (observed in 1995) we can place a  $3 - \sigma$  upper limit on PV Ceph’s proper motion of  $33 \text{ km s}^{-1}$  —too large to constrain the source-motion scenario proposed here. Happily, the wealth of upcoming precision astrometry missions (e.g. SIM, GAIA) should allow for a statistical sample of the motions of young and forming stars.

#### 4.2. “Matching” Cores and Stars

Ever since it was appreciated that stars form in the “dense cores” of molecular clouds (Myers & Benson 1983; Beichman et al. 1986), it has seemed puzzling that very few stars appear to be centered, alone in a blob of dense gas. Instead, it is generally true that one finds many young stars where one finds copious amounts of dense gas. Sometimes, especially for very young stars forming alone, it is easy to associate a star and its host core, but even in those cases, the star is often off-center with respect to gas features at  $\sim 0.1 \text{ pc}$  scales. In clusters, it is nearly impossible to associate a single star with a single core (e.g. Lada 1992), and there is also evidence that stars slowly diffuse out from the active part of the cluster as they form (Herbig 1998).

The “typical” velocity dispersion of molecular gas on 0.1 to 1 pc scales is of order  $1 \text{ km s}^{-1}$ . Moving at  $1 \text{ km s}^{-1}$ , it would take a star 100,000 years to go beyond the boundary of a core with radius 0.1 pc. Given these numbers, one can imagine a *slow* diffusion of stars out of their host cores, but not many cases of way-off-center stars after just, the typical “dynamical” time of a (young!) HH flow (10,000 years).

If, instead, velocities of  $1 \text{ km s}^{-1}$  were still typical in the gas, but some significant

fraction of stars —say those that had been ejected from higher-order systems very early in their creation— were moving at a range of higher velocities, one could expect many failed star-core associations. One can even imagine estimating the typical stellar velocity from star-core offsets —but that’s only possible if one can identify a star’s place of birth. Surely, this was not an easy task for PV Ceph!

#### *4.2.1. Estimating Star Formation Efficiency: What is the Right Reservoir of “Star-Forming” Gas?*

Star formation efficiency is typically calculated by dividing the stellar output of some region by the gas mass in that region. How, though, should a “region” be defined? To take an extreme example, would PV Ceph and NGC 7023 have been thought of as from one “region” —likely not.

We suggest here that further thought needs to be given to (spatially) lost generations of (still young) stars when calculating the star forming efficiency of molecular clouds. It may only be possible to do these calculations on very large scales —meaning that prior estimates of star formation efficiency, especially of regional variations, may be misleading. A similar suggestion has been made by Feigelson (1996) based on evidence for a distributed population of weak-lined T-Tauri stars found far from their birthplaces. The evidence for the youth of these stars has been called into question, but the suggestion that emigrées need counting when calculating star formation efficiency by census is surely correct.

### **4.3. Nagging Questions**

If PV Ceph formed  $\sim 10^5$  years ago in NGC 7023, how does it have such an extensive molecular outflow, now? Examining AGa, Figure 5, one sees that “first encounter” of PV

Ceph, moving at  $\sim 20 \text{ km s}^{-1}$ , and the molecular cloud in which it now finds itself, would have been about 35,000 years ago (0.7 pc to the East of its current position). As shown by our analysis of the outflow in §2, which suggests that the current features were created within the past 10,000 years, this is a perfectly reasonable time constraint, but it does beg the question of what PV Ceph was doing while it cruised through the vast expanse of nearly lower density material between it and NGC 7023. Did it start forming in the cluster, then go dormant, and then get re-invigorated when it entered its current host molecular cloud?

The Bondi-Hoyle analysis in §2.2.2 implies that only a very small blob ( $\sim 0.001 \text{ pc}$ ) of material could have traveled with PV Ceph from NGC 7023 at  $20 \text{ km s}^{-1}$ . Is it possible that PV Ceph took a disk with it, and that the outflow/disk system just started “working” (again?) as PV Ceph entered its current molecular cloud? One interesting point is that the clockwise rotation of the outflow axis evident in Figure 1 implies that PV Ceph’s disk has changed its orientation over the past 10,000 years to be parallel to its (nearly) E-W current direction of motion.<sup>18</sup> This could easily be an accident, but investigating this “coincidence” further is a nagging question nonetheless.

## 5. Summary

While the evidence for PV Ceph moving at roughly  $20 \text{ km s}^{-1}$  is all circumstantial, it comes from independent observations, and it is strong. In §2.1.1, we show that a straightforward “plasmon” model of gas deceleration can readily explain the currently observed positions of the optically-detected HH knots in the PV Ceph flow (see §2.1), but only if PV Ceph itself is moving at roughly  $22 \text{ km s}^{-1}$ . In §2.2, we show evidence for a

---

<sup>18</sup>We credit Dimitar Sasselov for causing us to wonder about the significance of alignment of PV Ceph’s disk and its direction of motion.

trail of redshifted molecular gas, detected in both  $^{12}\text{CO}$  and  $^{13}\text{CO}$ , at both low and high resolution, left behind in the wake of PV Ceph as it moves along a mostly E-W path with a small component away from us. Using HST observations of PV Ceph, we find the current jet direction to be very close to N-S. We compare this orientation with that of the wiggling highest-velocity molecular jet observed at high resolution and find that the offset between the optical and molecular jet directions is best explained if PV Ceph is moving—at  $21 \text{ km s}^{-1}$  from E to W (§2.3). We emphasize that the HST and IRAM molecular-line observations that give this velocity are independent from the large-scale optical imaging that implies  $22 \text{ km s}^{-1}$  based on the HH knot geometry.

In Figure 7, we summarize the recent history of PV Ceph implied by our findings. The Figure emphasizes that the knots in an HH flow from a young star can acquire a very noticeable velocity in the direction of the star’s motion, if that star is moving rapidly.<sup>19</sup>

A velocity of  $\sim 20 \text{ km s}^{-1}$  for a young star is unlikely to arise randomly, and is much more likely caused by a dynamical ejection (§3). In analyzing PV Ceph’s environs, we find NGC 7023 —10 pc from PV Ceph in projection— to be the nearest young cluster from which it may have been ejected. Astonishingly, we find that the back-track of PV Ceph’s motion, in all three spatial directions, seems to point quite precisely to NGC 7023. Furthermore, we find a dark rift in NGC 7023’s nebulosity that aligns eerily well with the exit path PV Ceph would have taken from the cluster (Figure 6).

It would take PV Ceph hundreds of thousands of years to travel from NGC 7023 to its

---

<sup>19</sup>Figure 7 is based on a movie prepared for a presentation of these results at the January 2004 meeting of the American Astronomical Society. The movie showing the evolution of the knots in time, along with other information on PV Ceph, is available through: [cfa-www.harvard.edu/~agoodman/Presentations/aas04PVCeph/](http://cfa-www.harvard.edu/~agoodman/Presentations/aas04PVCeph/).

current location. Most of the space in-between is of much lower density than either NGC 7023 or the cloud now hosting PV Ceph. What, exactly, PV Ceph would have been doing during the trip (e.g. did it have a disk? an outflow? was it dormant?) remains a difficult and fascinating, but open question.

If it turns out that this seemingly bizarre story where PV Ceph was ejected from NGC 7023 is right, we may need to reconsider the formation histories of some other young stars, too. To date, we know of seven examples, including PV Ceph, of pre-main-sequence stars moving at  $\gg 10 \text{ km s}^{-1}$  (§4.1). All of these speeders have been caught serendipitously, and we suggest that a systematic search for high-velocity young stars might yield dramatic results. If it turns out that speeding is a common offense—as many modern numerical simulations of the star formation process would imply—calculations of star formation efficiency in molecular clouds, and perhaps even of the stellar initial mass function, will need to be revisited.

## 6. Acknowledgements

This paper was initially intended to be a short “Letter,” based just on the geometric arguments in §2.1. The more people we talked with about the work, though, the more interesting—and more complex—the questions associated with it became. The people responsible for the happy expansion of this work include: John Bally, Ian Bonnell, Cathie Clarke, Bruce Elmegreen, Lee Hartmann, Charles Lada, Richard Larson, Laurent Loinard, Lucas Macri, Douglas Richstone, Phil Myers, Ramesh Narayan, Eve Ostriker, Alex Raga, Bo Reipurth, Luis Rodríguez, Edward Schwartz, Dimitar Sasselov, James Stone, and James Yorke. We are deeply grateful to have had their thoughts, questions, and insights. We are also indebted to Deborah Padgett and Karl Stapelfeldt for giving us their team’s HST images of PV Ceph in advance of their publication (Padgett, Brandner, Stapelfeldt, & Krist

1999). We thank the anonymous referee for pointing us to the highly relevant work on bent jets in clusters that we had somehow overlooked in our original submission. AG is grateful to the Yale University Astronomy Department for their kind hospitality while much of this work was in progress. HGA would also like to acknowledge the partial support from NSF grant AST-9981546.

## REFERENCES

- Arce, H. G. & Goodman, A. A. 2001, *ApJ*, 551, L171.
- Arce, H. G. & Goodman, A. A. 2002a, *ApJ*, 575, 911 [AGa]
- Arce, H. G. & Goodman, A. A. 2002b, *ApJ*, 575, 928 [AGb]
- Aveni, A. F. & Hunter, J. H. 1969, *AJ*, 74, 1021
- Beichman, C. A., Myers, P. C., Emerson, J. P., Harris, S., Mathieu, R., Benson, P. J., & Jennings, R. E. 1986, *ApJ*, 307, 337
- Bally, J., Devine, D., & Alten, V. 1996, *ApJ*, 473, 921
- Bally, J., & Reipurth, B. 2001, *ApJ*, 546, 299
- Bate, M. R., Bonnell, I. A., & Bromm, V. 2002, *MNRAS*, 336, 705
- Bate, M. R., Bonnell, I. A., & Bromm, V. 2003, *MNRAS*, 339, 577
- Blaauw, A. 1961, *Bull. Astron. Inst. Netherlands*, 15, 265
- Bonnell, I., Bate, M., Clarke, C. & Pringle, J. 2001, *MNRAS*, 323, 785
- Bonnell, I. A., Bate, M. R., & Vine, S. G. 2003, *MNRAS*, 343, 413
- Cabrit, S. & Raga, A. 2000, *A&A*, 354, 667
- Clarke, C. J. & Pringle, J. E. 1992, *MNRAS*, 255, 423
- Cantó, J. & Raga, A. C. 1995, *MNRAS*, 277, 1120
- Cantó, J., Espresate, J., Raga, A. C., & D'Alessio, P. 1998, *MNRAS*, 296, 1041
- Cohen, M., Kuhl, L. V., Spinrad, H., & Harlan, E. A. 1981, *ApJ*, 245, 920

- de La Fuente Marcos, R. 1997, *A&A*, 322, 764
- Devine, D. 1997, Ph.D. thesis, Univ. Colorado
- Devine, D., Bally, J., Reipurth, B., & Heathcote, S. 1997, *AJ*, 114, 2095
- De Young, D.S. & Axford, W.I. 1967, *Nature*, 216, 129
- Elmegreen, D. M. & Elmegreen, B. G. 1978, *ApJ*, 220, 510
- Feigelson, E. D. 1996, *ApJ*, 468, 306
- Frink, S., Röser, S., Neuhäuser, R., & Sterzik, M. F. 1997, *A&A*, 325, 613
- Fuente, A., Martin-Pintado, J., Bachiller, R., Neri, R., & Palla, F. 1998, *A&A*, 334, 253
- Fuente, A., Martin-Pintado, J., Rodriguez-Franco, A., & Moriarty-Schieven, G. D. 1998, *A&A*, 339, 575
- Furlan, E., Forrest, W. J., Watson, D. M., Uchida, K. I., Brandl, B. R., Keller, L. D., & Herter, T. L. 2003, *ApJ*, 596, L87
- Gerin, M., Phillips, T. G., Keene, J., Betz, A. L., & Boreiko, R. T. 1998, *ApJ*, 500, 329
- Gies, D. R. & Bolton, C. T. 1986, *ApJS*, 61, 419
- Gomez, M., Kenyon, S. J., & Whitney, B. A. 1997, *AJ*, 114, 265
- Gyulbudagyan, A. L. & Magakyan, T. Y. 1977, *Pis ma Astronomicheskii Zhurnal*, 3, 113
- Herbig, G. H. 1998, *ApJ*, 497, 736
- Hoogerwerf, R., de Bruijne, J. H. J., & de Zeeuw, P. T. 2001, *A&A*, 365, 49
- Jones, B. F. & Herbig, G. H. 1979, *AJ*, 84, 1872

- Kiseleva, L. G., Colin, J., Dauphole, B., & Eggleton, P. 1998, MNRAS, 301, 759
- Kroupa, P. 1998, MNRAS, 298, 231
- Lada, E. A. 1992, ApJ, 393, L25
- Leonard, P. J. T. & Duncan, M. J. 1990, AJ, 99, 608
- Li, W., Evans, N. J., Harvey, P. M., & Colome, C. 1994, ApJ, 433, 199
- Lim, A. J. & Raga, A. C. 1998, MNRAS, 298, 871
- Loinard, L., Rodríguez, L. F., & Rodríguez, M. I. 2003, ApJ, 587, L47
- Loinard, L. 2002, Revista Mexicana de Astronomia y Astrofisica, 38, 61
- Masciadri, E. & Raga, A. C. 2001, AJ, 121, 408
- Megeath, S.T. et al. 2004, BAAS, 35, 1244.
- Mendoza V., E. E. 1958, ApJ, 128, 207
- Myers, P. C. & Benson, P. J. 1983, ApJ, 266, 309
- Noriega-Crespo, A. & Garnavich, P. M. 2001, AJ, 122, 3317.
- Padgett, D. L., Brandner, W., Stapelfeldt, K. R., & Krist, J. E. 1999, BAAS, 31, 1489
- Perryman, M. A. C. et al. 1997, A&A, 323, L49
- Plambeck, R. L., Wright, M. C. H., Mundy, L. G., & Looney, L. W. 1995, ApJ, 455, L189
- Raga, A. C., Noriega-Crespo, A., Reipurth, B., Garnavich, P. M., Heathcote, S., Böhm, K. H., & Curiel, S. 2002, ApJ, 565, L29
- Reipurth, B. 2000, AJ, 120, 3177

- Reipurth, B. & Bally, J. 2001, *ARA&A*, 39, 403.
- Reipurth, B., Bally, J., & Devine, D. 1997, *AJ*, 114, 2708.
- Ridge, N. A., Wilson, T. L., Megeath, S. T., Allen, L. E., & Myers, P. C. 2003, *AJ*, 126, 286
- Sartori, M. J., Lépine, J. R. D., & Dias, W. S. 2003, *A&A*, 404, 913
- Sterzik, M. F. & Durisen, R. H. 1995, *A&A*, 304, L9
- Stone, R. C. 1991, *AJ*, 102, 333
- Strom, S. E., Strom, K. M., Yost, J., Carrasco, L., & Grasdalen, G. 1972, *ApJ*, 173, 353
- Watt, G. D., Burton, W. B., Choe, S.-U., & Liszt, H. S. 1986, *A&A*, 163, 194
- Valtonen, M. & Mikkola, S. 1991, *ARA&A*, 29, 9

Fig. 1.— The main (central) panel shows the integrated intensity of the  $^{12}\text{CO}(2-1)$  PV Ceph outflow (from AGa) superimposed on a wide-field  $\text{H}\alpha + \text{S}[\text{II}]$  CCD image (from Reipurth et al. 1997). Blue (red) contours denote the blueshifted (redshifted) lobe of the molecular outflow. The position of the HH knots and that of PV Ceph are shown. The three colored, straight, lines (shown in all panels) connect pairs of HH knots from the same ejection event, but opposing directions, from the star. The orange line connects the oldest ejection event (the HH 315 C-F pair), the green line connects the HH 315 B-E event, and the blue line connects the HH 315 A-D event. The circle in each of the three colored lines (shown in all panels) denotes the halfway point between the current positions of the given HH knot pair. The upper-left panel shows the redshifted  $^{13}\text{CO}(1-0)$  emission ( $3.15 < v_{LSR} < 3.71 \text{ km s}^{-1}$ , from AGb) superimposed on the same optical image as the main panel, but only covering a small ( $2' \times 2'$ ) region surrounding PV Ceph. The middle-left panel shows the HST/WFPC2 image of the region around PV Ceph (from Padgett, personal communication). The two panels on the right show the high-resolution  $^{12}\text{CO}(2-1)$  redshifted outflow emission (from AGb). The upper panel shows the “less” redshifted outflow integrated intensity ( $3.16 < v_{LSR} < 4.15 \text{ km s}^{-1}$ ) and the lower panel shows the “more” redshifted outflow integrated intensity ( $4.15 < v_{LSR} < 6.46 \text{ km s}^{-1}$ ). The solid yellow line in these two panels shows the N-S position angle of the current PV Ceph outflow axis (see text).

Fig. 2.— Plot showing the loci of possible HH knot positions, in a reference frame tied to the moving source, using the plasmon model (see text). The (0,0) position corresponds to the current position of the outflow source. The different curves represent the results of the model for different outflow source velocities (each curve is labeled with the velocity of the outflow source). The rest of the parameter values for the three different curves shown are identical, and are shown in Table 2. The black dots represent the observed position of the three different HH knot pairs of the HH 315 flow, in this coordinate system. Notice that the model with a source velocity of  $22 \text{ km s}^{-1}$  (middle curve) fits very well the observed knot

positions in the PV Ceph flow.

Fig. 3.— (*Top.*) Plot of “dynamical time” over real elapsed time vs. the distance of the HH knot from the emitting source. The dynamical time of an HH knot is defined as the observed distance of the knot over the observed velocity of the knot. (*Bottom.*) Plot of the velocity of the knot along the jet direction vs. the distance of the HH knot from the emitting source. In both panels the curve represents the results of the moving-source plasmon model (see text) using the parameters in Table 2. The gray filled circles show where the different HH knot pairs of the HH 315 flow would lie on the curves at the deprojected distances of the observed knots. Each of the three HH knot pairs are labeled.

Fig. 4.— Plot representing the amount of gas that might move along with a speeding protostar, using the modified Bondi-Hoyle method (see text). Diagonal solid lines in the log-log plot, show the relation between  $GM_*/R_{BH}$  and the Bondi-Hoyle accretion radius ( $R_{BH}$ ) for stars with different masses. The two dotted horizontal lines show where different values of  $\sigma_{eff}$  lie on the plot. The filled circle shows an estimate of where PV Ceph would lie on the plot, with  $\sigma_{eff} \sim (5 \text{ km s}^{-1})^2$  and  $M_* \sim 7 M_\odot$ . The dashed vertical line indicates the estimated value of  $R_{BH}$  for PV Ceph ( $R_{BH} \sim 0.001 \text{ pc}$ ).

Fig. 5.— (*Left.*) Plot of the high-resolution  $^{12}\text{CO}(2-1)$  redshifted outflow lobe emission centroid position (adapted from Figure 18 in AGb). The dark line shows the linear fit to the points. Distances are given in terms of pixels and arcseconds from the map edge. The gray arrows show the velocity vectors of the jet ( $v_{jet}$ ) and of the star ( $v_*$ ). (*Right.*) Same plot as on the left panel, but corrected for the slope (linear fit) shown on the left panel. Distances are shown in AU and arcseconds from the source. The sinusoidal fit to the points is also shown.

Fig. 6.— Main (right) panel shows the  $100\mu\text{m}$  IRAS image of the region near PV Ceph and the young stellar cluster NGC 7023. Superimposed on the IRAS image, at the position of NGC 7023, is a DSS image of NGC 7023. This same DSS image is blown-up and shown on the upper-left panel. The magenta arrow in the main panel is an extension towards the east of the presumed direction of motion of PV Ceph (from Figure 1), and corresponds to the magenta line in the blown-up DSS image (upper-left panel). The white star symbols show the position of two IRAS sources (possibly protostars) east of PV Ceph, IRAS 20495+6757 and IRAS 20514+6801. On the left panel, a dark lane in the DSS image of NGC 7023 is identified as a possible gap produced by the ejection of PV Ceph from NGC 7023 (see text).

Fig. 7.— Schematic illustration of PV Ceph’s history. For each pair of HH knots, small colored diamonds show the location, in time steps of 500 years, of the tip of a jet emitted from the point drawn as an “explosion” of the same color. The relevant portions of Figure 1 are repeated in the background here, and the diamonds are color-coded to match the connecting-line for each pair of knots. Larger diamonds emphasize the tips of those connecting lines, showing current HH knot positions. The plasmon model described in §2.1.1 was used to create this figure, but the ejection angle for each pair of knots has been rotated by hand to match the observed positions of the knots. Taken literally, this figure implies that the outermost pair of knots was emitted 9500 years ago, the middle pair 4700 years ago, and the innermost pair 2200 years ago, while PV Ceph traveled at  $22 \text{ km s}^{-1}$ . A movie showing the evolution of the knots in time is available through: [cfa-www.harvard.edu/~agoodman/Presentations/aas04PVCeph/](http://cfa-www.harvard.edu/~agoodman/Presentations/aas04PVCeph/).

Table 1. Observed Positions of Knots in the PV Ceph Flow

	Pair			
	Designation	$R_{knot}^a$	$R_{source}^b$	P.A.
	HH 315	[pc]	[pc]	[deg. E of N]
Outermost Knots	C-F	1.30	0.100	144
Middle Knots	B-E	0.90	0.056	156
Innermost Knots	A-D	0.52	—	159

<sup>a</sup> $R_{knot}$  is one-half of the distance between the knot pair listed, measured on the plane of the sky, assuming a distance to PV Ceph of 500 pc.

<sup>b</sup> $R_{source}$  is the plane-of-the-sky distance between the bisector of a line joining each knot pair listed and the current position of PV Ceph (which is the same, to within our measurement error, as the current position of the A-D bisector), assuming a distance to PV Ceph of 500 pc.

<sup>c</sup>P.A. gives the angle East of North defined by the line joining each pair of knots (see Figure 1).

Table 2. Parameters Used in Plasmon Model of the PV Ceph Flow

---



---

Star velocity, in direction of its motion <sup>a</sup>	$v_* = 22 \text{ km s}^{-1}$
Inclination of star’s motion to sky plane <sup>b</sup>	$\phi_{star-sky} = 20^\circ$
Initial velocity of ejected blobs <sup>a</sup>	$v_j = 350 \text{ km s}^{-1}$
Inclination of blob ejection (jet) axis to sky plane <sup>b</sup>	$\phi_{flow-sky} = 45^\circ$
Initial angle between source motion and jet axis in $v_j - v_*$ plane <sup>c</sup>	$\theta_0 = 90^\circ$
Mass of each ejected blob <sup>b</sup>	$M = 3 \times 10^{-4} M_\odot$
Number density (of H <sub>2</sub> ) corresponding to $\rho_{amb}$ <sup>c</sup>	$n_{amb} = 1.50 \times 10^3 \text{ cm}^{-3}$
Velocity dispersion in ambient medium <sup>c</sup> (e.g., <sup>12</sup> CO)	$\sigma = 3.2 \text{ km s}^{-1}$
Geometric factor <sup>b</sup>	$\xi = 14$

---

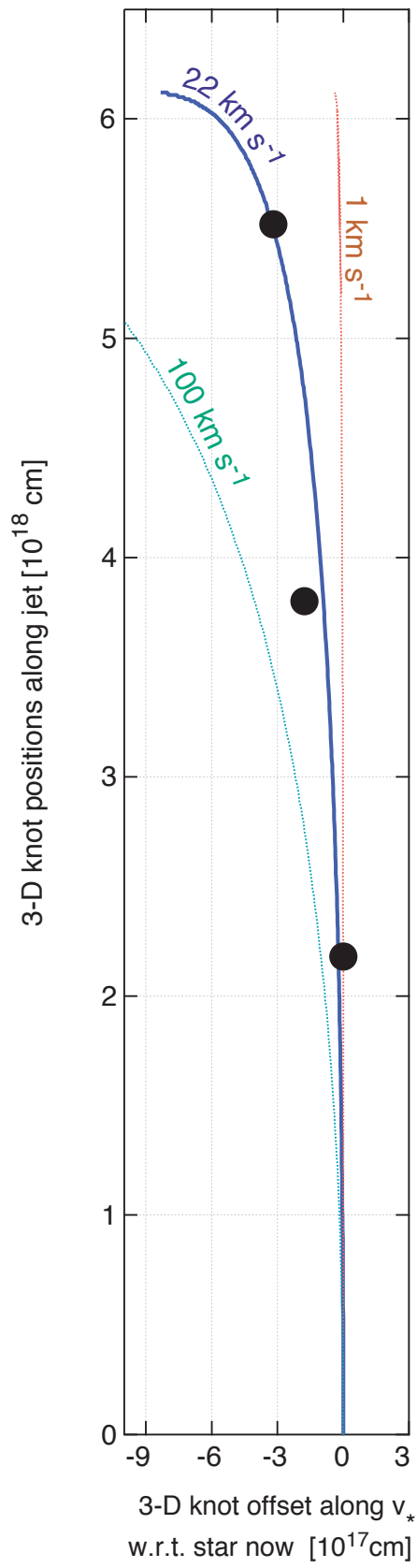
<sup>a</sup>Fitted parameter value.

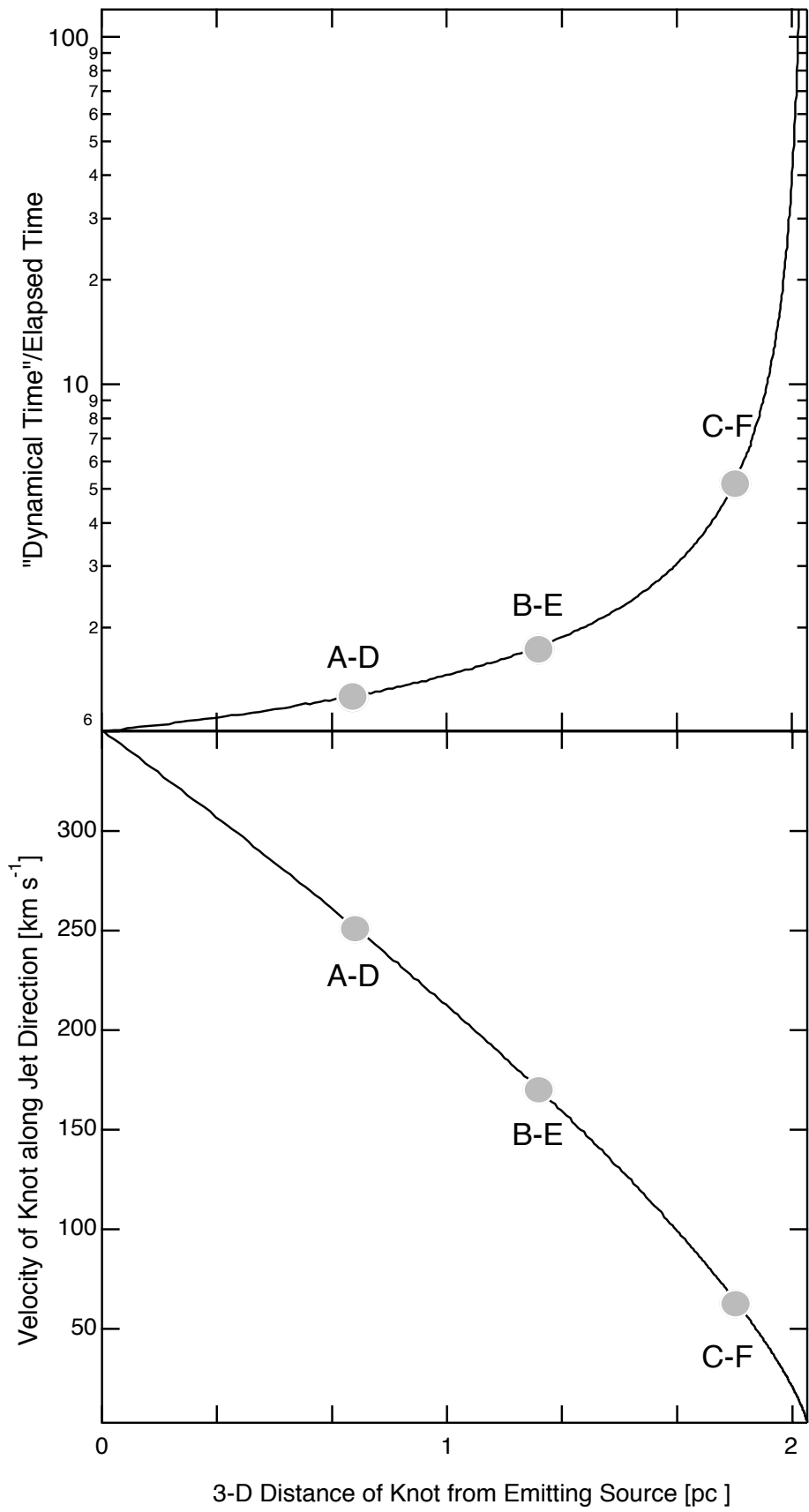
<sup>b</sup>Reasonable assumption made for parameter value.

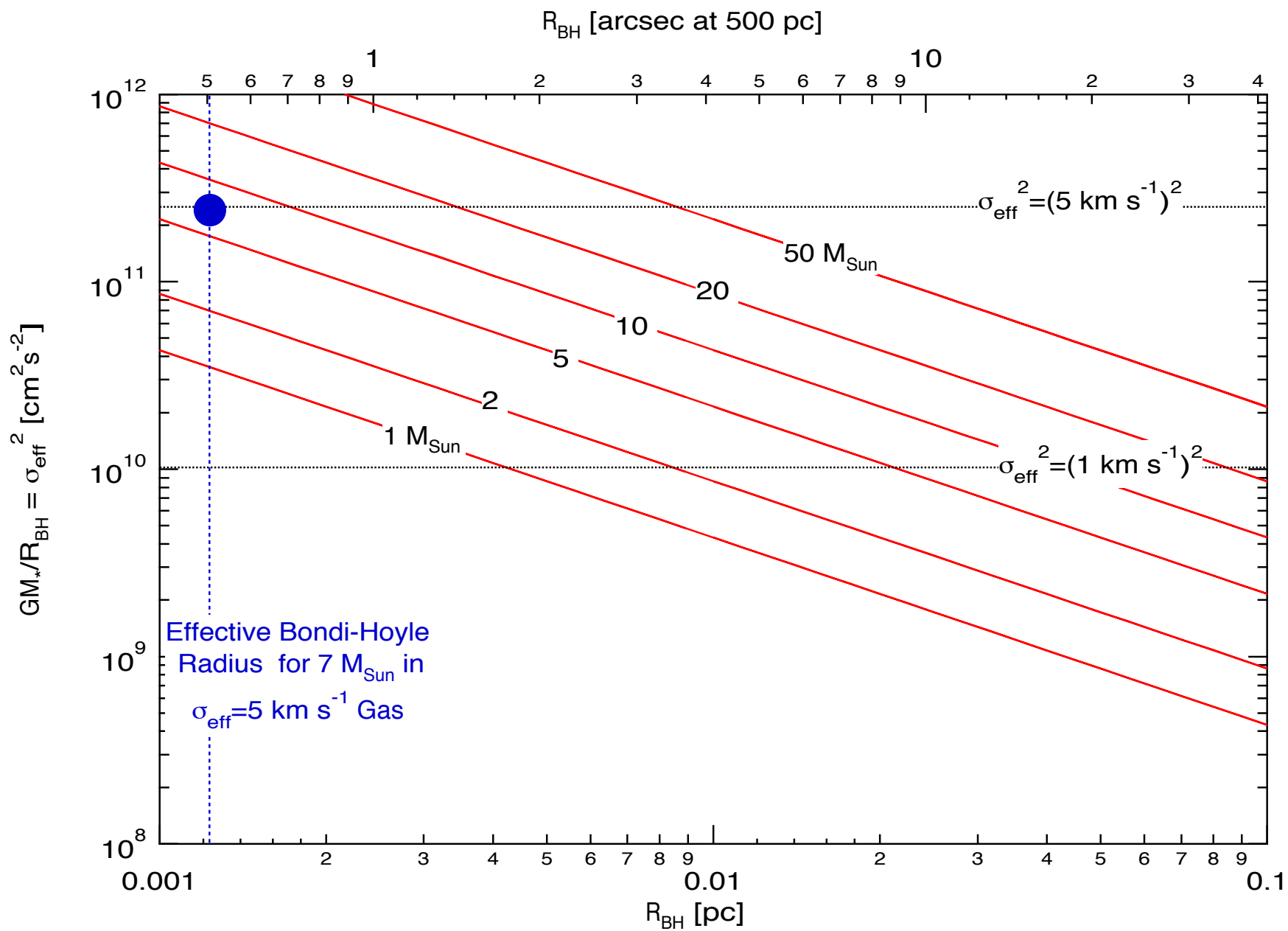
<sup>c</sup>Parameter value based on observations.

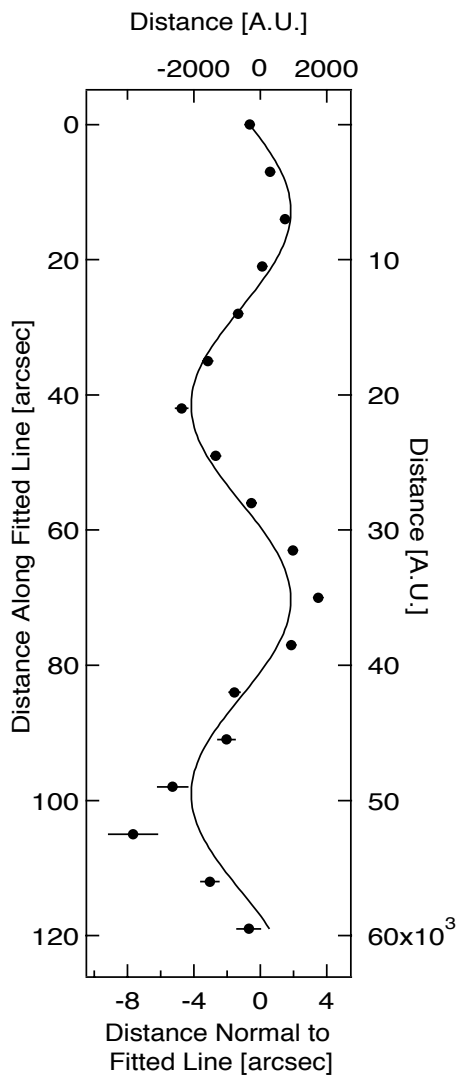
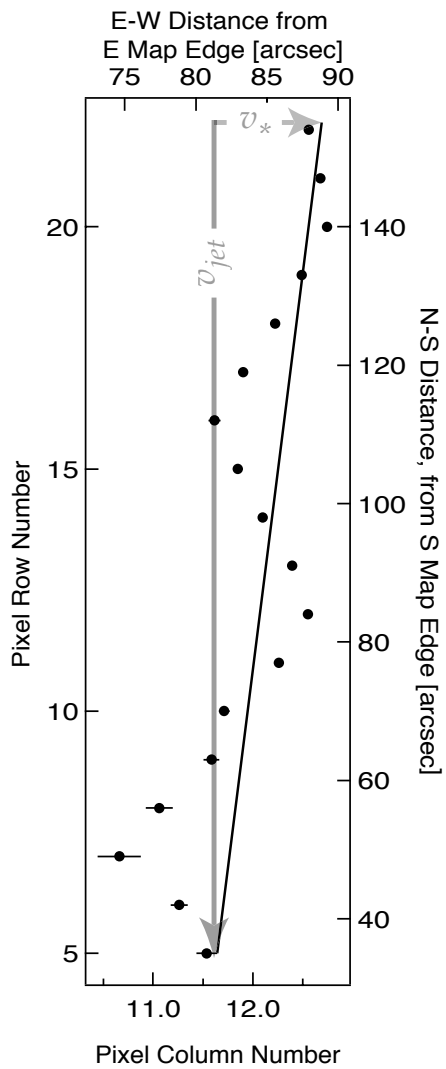
This figure "f1.gif" is available in "gif" format from:

<http://arxiv.org/ps/astro-ph/0401486v1>









This figure "f6.gif" is available in "gif" format from:

<http://arxiv.org/ps/astro-ph/0401486v1>

This figure "f7.gif" is available in "gif" format from:

<http://arxiv.org/ps/astro-ph/0401486v1>